

## Catalytic Properties of the Dioxomolybdenum Siloxide $\text{MoO}_2(\text{OSiPh}_3)_2$ and its 2,2'-Bipyridine Adduct $\text{MoO}_2(\text{OSiPh}_3)_2(\text{bpy})$

Sofia M. Bruno, Bernardo Monteiro, Maria Salete Balula, Catarina Lourenço, Anabela A. Valente, Martyn Pillinger, Paulo Ribeiro-Claro and Isabel S. Gonçalves \*

Department of Chemistry, CICECO, University of Aveiro, 3810-193 Aveiro, Portugal

\* Author to whom correspondence should be addressed; E-mail: igoncalves@dq.ua.pt

Received: 31 March 2006; in revised form: 10 April 2006 / Accepted: 10 April 2006 /

Published: 12 April 2006

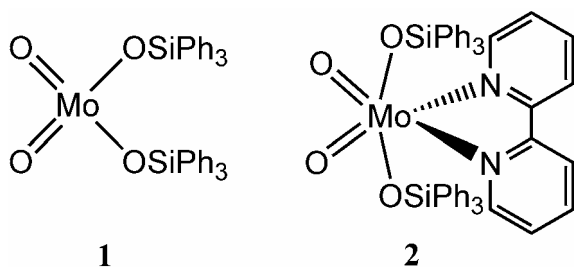
**Abstract:** The tetrahedral triphenylsiloxy complex  $\text{MoO}_2(\text{OSiPh}_3)_2$  (**1**) and its Lewis base adduct with 2,2'-bipyridine,  $\text{MoO}_2(\text{OSiPh}_3)_2(\text{bpy})$  (**2**), were prepared and characterised by IR/Raman spectroscopy, and thermogravimetric analysis. Both compounds catalyse the epoxidation of *cis*-cyclooctene at 55 °C using *tert*-butylhydroperoxide (*t*-BuOOH) as decane as the oxidant, giving 1,2-epoxycyclooctane as the only product. The best results were obtained in the absence of a co-solvent (other than the decane) or in the presence of 1,2-dichloroethane, while much lower activities were obtained when hexane or acetonitrile were added. With no co-solvent, catalyst **1** (initial activity 272 mol·mol<sub>Mo</sub><sup>-1</sup>·h<sup>-1</sup> for a catalyst:substrate: oxidant molar ratio of 1:100:150) is much more active than **2** (initial activity 12 mol·mol<sub>Mo</sub><sup>-1</sup>·h<sup>-1</sup>). The initial reaction rates showed first order dependence with respect to the initial concentration of olefin. With respect to the initial amount of oxidant, the rate order dependence for **1** (1.9) was higher than that for **2** (1.6). The dependence of the initial reaction rate on reaction temperature and initial amount of catalyst was also studied for both catalysts. The lower apparent activation energy of **1** (11 kcal·mol<sup>-1</sup>) as compared with **2** (20 kcal·mol<sup>-1</sup>) is in accordance with the higher activity of the former.

**Keywords:** Dioxomolybdenum(VI) complexes, siloxide ligands, Lewis base adducts, 2,2'-bipyridine, olefin epoxidation.

## Introduction

Over the last twenty years or so, several tetracoordinate (tetrahedral) dioxomolybdenum(VI) complexes of the type  $\text{MoO}_2(\text{OR})_2$  ( $\text{R} = \text{Me}, \text{Et}, n\text{-Pr}, \text{Ph}$  [1],  $t\text{-Bu}$ ,  $i\text{-Pr}$ ,  $\text{CH}_2t\text{-Bu}$  [2]) and  $\text{MoO}_2(\text{OSiR}_3)_2$  ( $\text{R} = t\text{-Bu}$  [3],  $\text{Ot-Bu}$  [4],  $\text{Ph}$  [5]) have been reported. The complexes with supporting siloxide ligands are of particular interest because they serve as models for isolated molybdenum atoms on a silica surface [6]. Surface-bound oxo-molybdenum species have attracted considerable attention in recent years because of their relevance to a variety of catalytic reactions, including the selective oxidations of alkanes, alkenes and alcohols [7,8]. Some of us recently reported on the catalytic activity of the triphenylsiloxy complex  $\text{MoO}_2(\text{OSiPh}_3)_2$  (**1**) for the liquid phase epoxidation of cyclic olefins using *tert*-butylhydroperoxide (*t*-BuOOH) as the mono-oxygen source [9]. Under homogeneous conditions (acetonitrile as co-solvent), the initial activity for the epoxidation of cyclooctene was about  $170 \text{ mol mol}_{\text{Mo}}^{-1} \text{ h}^{-1}$ , and the corresponding epoxide was the only observed product. The tetracoordinate (tetrahedral) oxomolybdenum complexes can form stable adducts with coordinating solvent molecules and Lewis base ligands, giving pentacoordinate complexes such as  $\text{MoO}_2(\text{OSi}(\text{Ot-Bu})_3)_2(\text{THF})$  [4] and  $\text{MoO}_2(\text{OSiPh}_3)_2(\text{PPh}_3)$  [5], and hexacoordinate (distorted-octahedral) complexes such as  $\text{MoO}_2(\text{OPh})_2(\text{py})_2$  [1],  $\text{MoO}_2(\text{OSiMe}_2t\text{-Bu})_2(\text{py})_2$  [1],  $\text{MoO}_2(\text{Ot-Bu})_2(\text{py})_2$  and  $\text{MoO}_2(\text{Ot-Bu})_2(\text{bpy})$  [2] ( $\text{py} = \text{pyridine}$ ,  $\text{bpy} = 2,2'\text{-bipyridine}$ ). The catalytic performance of these distorted-octahedral complexes has not been well studied, in contrast to Lewis base adducts of the type  $\text{MoO}_2\text{X}_2\text{L}$  ( $\text{X} = \text{Cl}, \text{Br}, \text{Me}$ ) bearing bidentate nitrogen-donor ligands ( $\text{L}$ ). The latter complexes are generally stable and, depending on the nature of  $\text{X}$  and  $\text{L}$ , can exhibit high activities and selectivities for olefin epoxidation [10,11]. In the present work, the novel complex  $\text{MoO}_2(\text{OSiPh}_3)_2(\text{bpy})$  has been prepared and characterized, and its catalytic behaviour has been compared with tetracoordinate (tetrahedral)  $\text{MoO}_2(\text{OSiPh}_3)_2$  (Figure 1).

**Figure 1.**



## Results and Discussion

### Synthesis and characterisation

The triphenylsiloxy complex  $\text{MoO}_2(\text{OSiPh}_3)_2$  (**1**) was prepared as described previously by the reaction of silver molybdate with two equivalents of  $\text{Ph}_3\text{SiCl}$  [5]. The adduct  $\text{MoO}_2(\text{OSiPh}_3)_2(\text{bpy})$  (**2**) was obtained either by treatment of a solution of previously prepared and isolated **1** with one equivalent of 2,2'-bipyridine, or directly in one step by the addition of bpy at the end of the reaction used to prepare **1**. Compounds **1** and **2** were characterised by elemental analysis,  $^1\text{H-NMR}$ , IR and Raman spectroscopy, and thermogravimetric analysis. The assignment of the vibrational spectra was

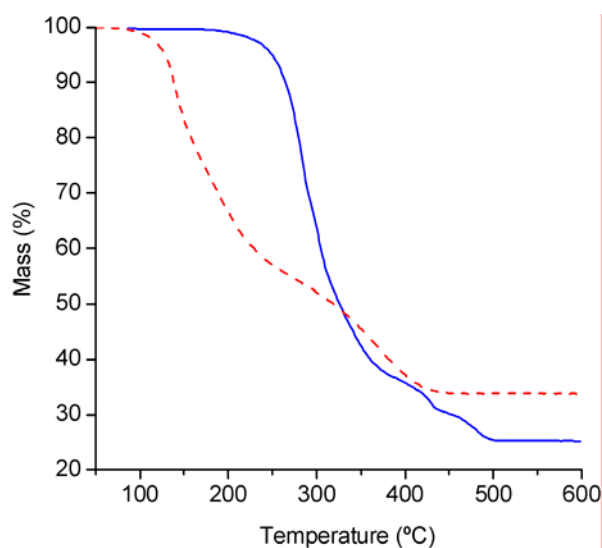
supported by *ab initio* calculations (Table 1). Molybdenum(VI) complexes with the *cis*-dioxo unit typically show two very strong IR peaks in the range 905–940 cm<sup>−1</sup> [11], assigned to the Mo=O stretching modes. In the case of the starting material, Na<sub>2</sub>MoO<sub>4</sub>·2H<sub>2</sub>O, strong bands for the Mo=O stretching modes are observed in the IR spectrum at 897 and 834 cm<sup>−1</sup>. These bands are shifted to higher frequencies (948 and 932 cm<sup>−1</sup>) for compound **1**, indicating a strengthening of the Mo=O bonds due to the formation of the O–SiPh<sub>3</sub> bonds. For the Mo–O bond, only a very weak band at 356 cm<sup>−1</sup> is observed, assigned to symmetric stretching. Compound **2** exhibits a pair of weak bands at 170 and 155 cm<sup>−1</sup> in the Raman spectrum, attributed to Mo–N asymmetric and symmetric stretching, respectively. As expected, the bidentate coordination of 2,2'-bipyridine, which implies a change from distorted tetrahedral to distorted octahedral geometry, weakens the MoO<sub>4</sub> bonds of the complex. As shown in Table 1, the Mo=O bands are shifted to lower frequencies and in the Raman spectrum the Mo=O<sub>sym</sub> is not observed. In contrast to compound **1**, the asymmetric stretching band for the Mo–O bond appears with medium intensity at 377 cm<sup>−1</sup>, while the symmetric stretching band is not observed.

**Table 1.** Selected IR and Raman stretching frequencies of Na<sub>2</sub>MoO<sub>4</sub>·2H<sub>2</sub>O, MoO<sub>2</sub>(OSiPh<sub>3</sub>)<sub>2</sub> (**1**) and MoO<sub>2</sub>(OSiPh<sub>3</sub>)<sub>2</sub>(bpy) (**2**), and calculated (B3LYP) frequencies of the three compounds.

Compound	Calcd <sup>a</sup>	IR (cm <sup>−1</sup> )	Raman (cm <sup>−1</sup> )	Assignment
Na <sub>2</sub> MoO <sub>4</sub> ·2H <sub>2</sub> O	838	897	896	vMoO <sub>4</sub> unit
	802	834	834	
MoO <sub>2</sub> (OSiPh <sub>3</sub> ) <sub>2</sub> ( <b>1</b> )	948	948m	949vw	v <sub>sym</sub> (Mo=O)
	892	932m	933vw	v <sub>asym</sub> (Mo=O)
	550	—	—	v <sub>asym</sub> (Mo–O) <sup>b</sup>
	439	356vw	358w	v <sub>sym</sub> (Mo–O) <sup>b</sup>
MoO <sub>2</sub> (OSiPh <sub>3</sub> ) <sub>2</sub> (bpy) ( <b>2</b> )	944	933vs	—	v <sub>sym</sub> (Mo=O)
	913	908vs	909vs	v <sub>asym</sub> (Mo=O)
	361	377m	378w	v <sub>asym</sub> (Mo–O)
	345	—	—	v <sub>sym</sub> (Mo–O)
	143	—	170w	v <sub>asym</sub> (Mo–N)
	141	—	155w	v <sub>sym</sub> (Mo–N)

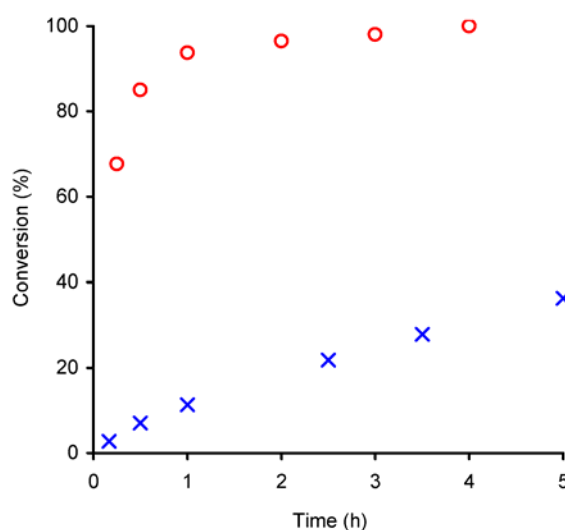
<sup>a</sup> Scaled values (scale factor = 0.961). <sup>b</sup> Highly mixed with O–Si stretching and Mo–O–Si bending modes. Abbreviations: vs = very strong, vw = very weak, m = medium, w = weak.

Thermogravimetric analysis under air (Figure 2) showed that compound **2** is significantly more stable than **1**. The tetrahedral complex **1** decomposes in two main steps from 80 to 440 °C, with 45% mass loss in the temperature range 80–270 °C, and 21% mass loss in the temperature range 270–440 °C. The observed ceramic yield at 600 °C is 33.8%, which is 5.1% lower than the calculated yield for MoO<sub>3</sub>·2SiO<sub>2</sub> (38.9%). The TGA results for **2** reflect a higher onset temperature of ca. 180 °C and a weight loss that is complete by 500 °C. The ceramic yield of 25% is 6.6% lower than that calculated for stoichiometric formation of MoO<sub>3</sub>·2SiO<sub>2</sub> (31.6%).

**Figure 2.** TGA curves of  $\text{MoO}_2(\text{OSiPh}_3)_2$  (**1**) (---) and  $\text{MoO}_2(\text{OSiPh}_3)_2(\text{bpy})$  (**2**) (—).

### Catalysis

The performance of compounds **1** and **2** as epoxidation catalysts was studied using *cis*-cyclooctene as a model substrate and *t*-BuOOH as oxygen donor. In a control experiment, carried out without catalyst, no reaction occurred, whereas in the presence of compounds **1** or **2** the conversion of cyclooctene produced 1,2-epoxycyclooctane as the only product, confirming the catalytic role of these compounds (Figure 3). Catalyst **1** (initial activity  $272 \text{ mol} \cdot \text{mol}_{\text{Mo}}^{-1} \cdot \text{h}^{-1}$ ) is much more active than **2** (initial activity  $12 \text{ mol} \cdot \text{mol}_{\text{Mo}}^{-1} \cdot \text{h}^{-1}$ ), and after 3 h the epoxide was obtained in quantitative yield in the presence of **1**, whereas for **2** the conversion was still only 22%. The observed catalytic activity of **2** is comparable to that of other distorted octahedral  $\text{Mo}^{\text{VI}}$  complexes of the type  $\text{MoO}_2\text{X}_2\text{L}$  ( $\text{X} = \text{Cl}, \text{Br}$ ) bearing bidentate N-donor ligands ( $\text{L}$ ) such as ethylenediiimine [10], bipyridine [11] and bipyrimidine [12].

**Figure 3.** Kinetics of the epoxidation of cyclooctene with *t*-BuOOH in decane at 55 °C, catalysed by compounds **1** (○) and **2** (×).

For compound **1**, the reaction rate decreases drastically with time. In general, the mechanisms proposed for *t*-BuOOH-based epoxidations of olefins with Mo<sup>VI</sup> complexes are heterolytic in nature, involving coordination of the oxidant to the metal centre (by the terminal oxygen of <sup>-</sup>OO*t*Bu in the case of the complexes MoO<sub>2</sub>X<sub>2</sub>L with X = Cl, Br or Me, and L = Lewis base N- or O-ligand), which acts as a Lewis acid thereby increasing the oxidising power of the peroxy group, and subsequently the olefin is epoxidised by nucleophilic attack on an electrophilic oxygen atom of the oxidising species [8,11]. The rapid decrease in the olefin conversion rate has been attributed to the formation of *tert*-butanol (*t*-BuOH), a by-product of the epoxidation, that acts as a competitor to *t*-BuOOH for coordination to the metal centre, leading to the formation of inactive species [11,12].

The solvent effect was studied for compounds **1** and **2** using 1,2-dichloroethane, *n*-hexane or acetonitrile, at 55 °C. No dependence of product selectivity on the solvent was observed. For both catalysts, conversion after 24 h reaction followed the order: no co-solvent ≥ dichloroethane > hexane > CH<sub>3</sub>CN, and TOF (calculated at 30 min) of cyclooctene epoxidation was highest without a co-solvent or with dichloroethane (Table 2). Acetonitrile has a negative effect on initial catalytic activity, which may be related to its ability to coordinate to the molybdenum centre. According to the above mechanistic assumptions, the competition between solvent and oxidant molecules for coordination to the metal centre may retard the reaction. However, the coordinating power of the solvent molecules does not solely explain the observed catalytic activity since when hexane, a non-coordinating solvent, is added to the reaction medium the epoxidation rate decreases significantly for both catalysts. Indeed, the TOF for **1** (calculated at 30 min) in the presence of CH<sub>3</sub>CN is higher than that observed for hexane. Hence, the dependence of catalytic activity on the type of solvent may be related to solvent-oxidant competitive ligand effects as well as changes in the solubility of the catalyst. The somewhat higher activity of **2** in dichloroethane may be associated with the higher catalyst solubility in the reaction medium.

**Table 2.** Catalytic activity of compounds **1** and **2** for cyclooctene epoxidation at 55 °C, using different co-solvents.

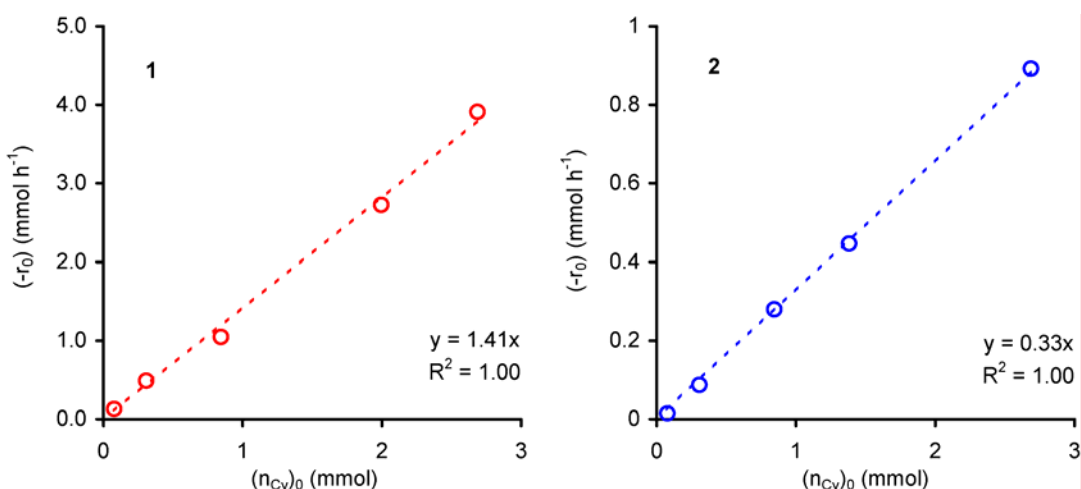
Solvent	Compound <b>1</b>		Compound <b>2</b>	
	TOF <sup>a</sup> (mol·mol <sub>Mo</sub> <sup>-1</sup> ·h <sup>-1</sup> )	Conv. <sup>b</sup> (%)	TOF <sup>a</sup> (mol·mol <sub>Mo</sub> <sup>-1</sup> ·h <sup>-1</sup> )	Conv. <sup>b</sup> (%)
none	170	100 <sup>c</sup>	14	74
1,2-dichloroethane	135	100 <sup>c</sup>	17	69
<i>n</i> -hexane	22	96	4	31
Acetonitrile	70	82	2	20

<sup>a</sup> Calculated at 30 min. <sup>b</sup> Calculated at 24 h. <sup>c</sup> Achieved within 4 h reaction.

The kinetics of the liquid-phase epoxidation of cyclooctene in the presence of **1** and **2** was further investigated using the method of initial rates (-r<sub>0</sub>), and keeping the total volume of the reaction mixture constant using decane (the solvent of the purchased *t*-BuOOH) as solvent.

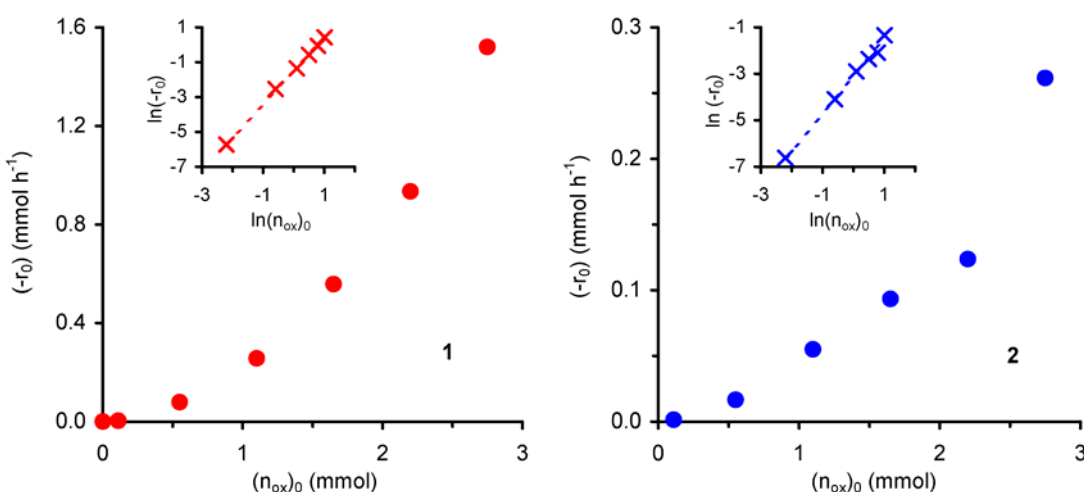
For all experiments cyclooctene epoxide was the only product. The dependence of the initial rate of cyclooctene conversion ( $-r_0$ ) on initial amount of cyclooctene ( $n_{Cy}^0$ ) was studied for initial concentrations of cyclooctene  $\leq 2 \text{ mol}\cdot\text{dm}^{-3}$  at 55 °C. For both compounds **1** and **2**, the plot of ( $-r_0$ ) versus ( $n_{Cy}^0$ ) is linear ( $R^2 = 0.99$ ), suggesting an apparent first order dependence with respect to cyclooctene concentration (Figure 4).

**Figure 4.** Dependence of the initial rate of cyclooctene epoxidation (with *t*-BuOOH in decane), catalysed by compounds **1** or **2**, as a function of the initial charge of cyclooctene.



The effect of the initial amount of oxidant ( $n_{ox}^0$ ) on the initial reaction rate ( $-r_0$ ) was studied for initial concentrations of *t*-BuOOH  $\leq 1.9 \text{ mol}\cdot\text{dm}^{-3}$  at 55 °C. Under the applied operating conditions, the reaction does not take place in the absence of *t*-BuOOH. The observed initial reaction rate increases with *t*-BuOOH concentration (Figure 5).

**Figure 5.** Dependence of the initial rate of cyclooctene epoxidation (with *t*-BuOOH in decane), catalysed by compounds **1** or **2**, as a function of the initial amount of peroxide.

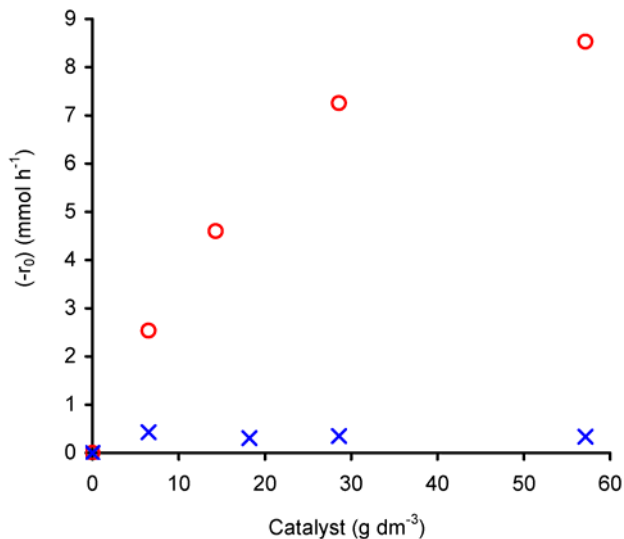


For both compounds the plot of  $\ln(-r_0)$  versus  $\ln(n_{\text{ox}})_0$  gives a straight line ( $R^2 = 0.99$ ) with slopes of 1.9 for **1** and 1.6 for **2**, corresponding to the apparent reaction orders with respect to *t*-BuOOH in the studied concentration range (insets of Figure 5). These values suggest that the catalytic epoxidation process includes a number of simultaneous and consecutive elementary reactions, in agreement with the above mechanistic assumptions. Accordingly, a higher initial concentration of *t*-BuOOH should increase the reaction rate by enhancing the *t*-BuOOH/*t*-BuOH molar ratio in the reaction medium, and thus the molar ratio between active (formed with *t*-BuOOH) and inactive (formed with *t*-BuOH) species.

The dependence of the initial conversion rate of cyclooctene on the reaction temperature (T) was studied in the temperature range of 35–70 °C. For all experiments cyclooctene oxide was the only observed product. For both compounds the observed initial reaction rate ( $-r_0$ ) increases with temperature (plot not shown), following a linear Arrhenius plot of  $\ln(-r_0)$  vs  $1/T$  ( $R^2 = 0.99$ , at constant reagents and catalyst concentrations). The apparent activation energy of **1** (11 kcal·mol<sup>-1</sup>) is lower than that of **2** (20 kcal·mol<sup>-1</sup>), as would be expected considering the higher activity of **1**.

The dependence of ( $-r_0$ ) on the initial amount of catalyst was studied in the range of 7–57 g<sub>cat</sub>·dm<sup>-3</sup>, at 55 °C (Figure 6). For compound **1** the reaction rate increases with catalyst charge. For W/L < 30 g<sub>cat</sub>·dm<sup>-3</sup>, the plot of  $\ln(-r_0)$  versus  $\ln(n_{\text{cat}})_0$  gives a straight line ( $R^2 = 0.99$ ) with a slope of 0.7 (not shown), corresponding to the apparent reaction order with respect to initial catalyst amount (( $n_{\text{cat}})_0$ ) in the studied concentration range. However, for charges greater than 30 g<sub>cat</sub>·dm<sup>-3</sup>, the differential rate law tends to become independent of the amount of catalyst, which may be due to a change in the controlling mechanism or catalyst solubility. On the other hand, at higher complex concentrations the productive utilisation of *t*-BuOOH may be levelled off due to its decomposition into *t*-BuOH and molecular oxygen.

**Figure 6.** Dependence of the initial rate of cyclooctene epoxidation (with *t*-BuOOH in decane), catalysed by compounds **1** (○) or **2** (×), as a function of the initial amount of charged catalyst.



Contrary to that observed for **1**, ( $-r_0$ ) for compound **2** is independent of the initial amount of catalyst, that is, it exhibits an apparent zero-order rate law with respect to the catalyst amount. Given the low

solubility of **2** in the reaction medium it is possible that the reaction rate is mainly governed by some soluble metal species and that increasing the concentration of catalyst does not further increase the amount of these active soluble species due to saturation of the solution.

Based on the above results, for the studied reaction temperature and intervals of initial concentrations, the initial rate ( $-r_0$ ) law of cyclooctene conversion in the presence of **2** may be expressed as  $(-r_0) = k(n_{\text{Cy}})_0(n_{\text{ox}})_0^{1.6}$ , where  $k$  represents the reaction rate constant. In the case of **1**, for  $W/L < 30 \text{ g}_{\text{cat}} \cdot \text{dm}^{-3}$  and for the specified limits of initial concentrations of reagents and reaction temperature, the initial rate ( $-r_0$ ) law in the presence of **1** may be expressed as  $(-r_0) = k(n_{\text{Cy}})_0(n_{\text{ox}})_0^{1.9}(n_{\text{cat}})_0^{0.7}$ , where  $k$  represents the reaction rate constant.

We have previously reported that **1** can be recycled without significant loss of activity, originating the same kinetic profiles as the fresh catalyst [9]. In this work the stability of **2** was studied in a similar fashion. After the first reaction cycle the catalyst was separated by centrifugation, washed several times with *n*-hexane and dried at room temperature prior to its reuse. As found for compound **1**, the conversion profiles for fresh and recovered **2** were similar, suggesting that these compounds are fairly stable under the applied reaction conditions.

## Conclusions

The present study has fully explored the promising behaviour of the tetrahedral complex  $\text{MoO}_2(\text{OSiPh}_3)_2$  (**1**) as a catalyst for the epoxidation of cyclooctene, using *tert*-butylhydroperoxide as the oxidant. Future work will be directed towards the applicability of the system to the epoxidation of other olefins as well as studying the effect of replacing the phenyl substituent by different groups. The introduction of the bidentate ligand 2,2'-bipyridine, which expands the coordination number to six to give a distorted octahedral complex (**2**), has a drastic and detrimental effect on catalytic performance. This may be due, in part, to the lower solubility of the Lewis base adduct in the reaction medium, and also steric hindrance should be less relevant for compound **1**. Coordination of one *t*-BuOOH molecule to compound **1**, giving a pentacoordinate species, is likely to be much more favourable than coordination of one oxidant molecule to compound **2**, which will necessitate the formation of a heptacoordinate species assuming that the Mo–N bonds remain intact.

## Acknowledgments

The authors are grateful to the FCT, OE and FEDER for funding (Project POCI/CTM/58507/2004). We also wish to thank the FCT for PhD (to BM) and post-doctoral (MSB) grants.

## Experimental

### General

All preparations and manipulations were carried out under nitrogen using standard Schlenk techniques. Solvents were dried by standard procedures (*n*-hexane with Na/benzophenone ketyl; acetonitrile and 1,2-dichloroethane with CaH<sub>2</sub>), distilled under nitrogen and kept over 4 Å or (for CH<sub>3</sub>CN) 3 Å molecular sieves. Silver molybdate (Ag<sub>2</sub>MoO<sub>4</sub>) was synthesized from silver nitrate (José M. Vaz Pereira) and sodium molybdate (Merck) and dried in vacuum at 60 °C for several hours prior

to use. 2,2'-Bipyridine (Merck), triphenylchlorosilane (Aldrich), *t*-BuOOH (5.5 M in decane, Aldrich) and acetone-d<sub>6</sub> (Aldrich) were purchased from commercial sources and used as received. Thermogravimetric analysis (TGA) was carried out under air using a Shimadzu TGA-50 system at a heating rate of 5 °C min<sup>-1</sup>. IR spectra were obtained as KBr pellets using a FTIR Mattson-7000 infrared spectrophotometer. Raman spectra were recorded on a Bruker RFS100/S FT instrument (Nd:YAG laser, 1064 nm excitation, InGaAs detector). <sup>1</sup>H-NMR spectra were obtained using a Bruker CXP 300 spectrometer. Gas chromatography was carried out on a Varian 3800 instrument equipped with a capillary column (SPB-5, 20 m × 0.25 mm) and a flame ionisation detector. Elemental analyses were performed at the University of Aveiro.

### Ab initio calculations

*Ab initio* calculations were performed using the G03w program package [13]. The fully optimised geometry, the harmonic vibrational frequencies, and the infrared and Raman intensities were obtained at the B3LYP level, using the Effective Core Potentials of Hay and Wadt [14] for the Mo atom and the valence double-zeta basis set of Dunning and Huzinaga [15] for the remaining atoms (Lanl2DZ basis set of G03). In order to improve the description of the Mo–O bonds, a *d* polarisation function ( $\xi = 0.85$ ) was added to the oxygen atoms. For the starting product, the calculations were performed using the fragment MoO<sub>4</sub><sup>2-</sup>. The calculated wavenumbers were scaled by a factor of 0.961 [16] before comparison with the experimental values.

### MoO<sub>2</sub>(OSiPh<sub>3</sub>)<sub>2</sub> (**1**)

Obtained in 86% yield using the published method [5]. IR (KBr):  $\nu = 3067\text{w}$ , 3049w, 3022w, 1961vw, 1890vw, 1822vw, 1773vw, 1588w, 1566vw, 1484w, 1440w, 1428s, 1383vw, 1330vw, 1304vw, 1261vw, 1187w, 1158vw, 1119vs, 1067vw, 1027vw, 1015vw, 997m, 948s, 932s, 888vs, 835s, 738m, 712vs, 697vs, 619vw, 576vw, 556w, 536vw, 512vs, 454vw, 431w, 356vw cm<sup>-1</sup>; Raman: 3052vs, 1590s, 1568m, 1190w, 1158w, 1107w, 1030m, 1001vs, 949vw, 933vw, 684w, 619w, 238w cm<sup>-1</sup>.

### MoO<sub>2</sub>(OSiPh<sub>3</sub>)<sub>2</sub>(bpy) (**2**)

A suspension of Ag<sub>2</sub>MoO<sub>4</sub> (0.67 g, 1.80 mmol) in 1,2-dichloroethane (35 mL) and CH<sub>3</sub>CN (3 mL) was stirred for 15 minutes. Ph<sub>3</sub>SiCl (1.06 g, 3.60 mmol) was then added, and the mixture was refluxed under nitrogen for 5 h. The solution was filtered at room temperature and treated with 2,2'-bipyridine (0.28 g, 1.80 mmol). After stirring for 2 h at room temperature, the solution was evaporated to dryness, and the resultant product washed with *n*-hexane (3 × 15 mL) and diethyl ether (2 × 15 mL) at <35 °C, and finally dried under reduced pressure for 3 h at 40 °C to give compound **2** as a white solid (1.15 g, 77%). Anal. Calcd for C<sub>46</sub>H<sub>38</sub>MoN<sub>2</sub>O<sub>4</sub>Si<sub>2</sub> (834.92): C, 66.17; H, 4.59; N, 3.36. Found: C, 65.39; H, 4.88; N, 3.53%; IR (KBr):  $\nu = 3063\text{m}$ , 3021w, 1960vw, 1896vw, 1821vw, 1603m, 1595m, 1588m, 1575w, 1565w, 1491w, 1482w, 1473m, 1441s, 1428vs, 1383w, 1329vw, 1313m, 1261w, 1244w, 1221vw, 1190w, 1172w, 1156w, 1114vs, 1058w, 1026m, 999m, 933vs, 908vs, 760m, 737s, 707vs, 700vs, 650m, 631m, 620vw, 552vw, 529m, 510vs, 452m, 436s, 377m, 341w, 305m cm<sup>-1</sup>; Raman:

3073s, 3047vs, 3025w, 1596vs, 1590vs, 1566s, 1492m, 1312s, 1281w, 1266w, 1185w, 1158m, 1107w, 1058w, 1032m, 1007vs, 998vs, 909vs, 768w, 682w, 620w, 378w, 255w, 240m, 213w, 199w, 170w, 155w cm<sup>-1</sup>; <sup>1</sup>H-NMR (300.13 MHz, 25 °C, acetone-d<sub>6</sub>): δ = 9.09–9.08 (m, py-H), 8.70–8.69 (m, py-H), 8.52–8.49 (m, py-H), 7.98–7.92 (m, py-H), 7.67–7.64 (m, Ph-H), 7.48–7.38 (m, Ph-H), 7.31–7.14 (m, py-H + Ph-H) ppm.

### Catalysis

The liquid-phase catalytic oxidations were carried out under air at 55 °C and atmospheric pressure in a reaction vessel equipped with a magnetic stirrer and immersed in a thermostated oil bath. Typically, a 1% molar ratio of free complex/substrate and a substrate/oxidant (*t*-BuOOH, 5.5 M in decane) molar ratio of 0.65 were used. The course of the reactions was monitored by GC.

### References

1. Kim, G.-S.; Huffman, D.; DeKock, C. W. *Inorg. Chem.* **1989**, *28*, 1279–1283.
2. Chisholm, M. H.; Folting, K.; Huffman, J. C.; Kirkpatrick, C. C. *Inorg. Chem.* **1984**, *23*, 1021–1037.
3. Weidenbruch, M.; Pierrard, C.; Pesel, H. Z. *Naturforsch.* **1978**, *33B*, 1468–1471.
4. Jarupatrakorn, J.; Coles, M. P.; Tilley, T. D. *Chem. Mater.* **2005**, *17*, 1818–1828.
5. Huang, M.; DeKock, C. W. *Inorg. Chem.* **1993**, *32*, 2287–2291.
6. Brisdon, B. J.; Mahon, M. F.; Rainford, C. C. *J. Chem. Soc., Dalton Trans.* **1998**, 3295–3299.
7. Ferreira, P.; Gonçalves, I. S.; Kühn, F. E.; Lopes, A. D.; Martins, M. A.; Pillinger, M.; Pina, A.; Rocha, J.; Romão, C. C.; Santos, A. M.; Santos, T. M.; Valente, A. A. *Eur. J. Inorg. Chem.* **2000**, 2263–2270, and references cited therein.
8. Nunes, C. D.; Valente, A. A.; Pillinger, M.; Rocha, J.; Gonçalves, I. S. *Chem. Eur. J.* **2003**, *9*, 4380–4390, and references cited therein.
9. Abrantes, M.; Valente, A. A.; Pillinger, M.; Gonçalves, I. S.; Rocha, J.; Romão, C. C. *Inorg. Chem. Commun.* **2002**, *5*, 1069–1072.
10. Petrovski, Ž.; Pillinger, M.; Valente, A. A.; Gonçalves, I. S.; Hazell, A.; Romão, C. C. *J. Mol. Catal. A: Chem.* **2005**, *227*, 67–73, and references cited therein.
11. Al-Ajlouni, A.; Valente, A. A.; Nunes, C. D.; Pillinger, M.; Santos, A. M.; Zhao, J.; Romão, C. C.; Gonçalves, I. S.; Kühn, F. E. *Eur. J. Inorg. Chem.* **2005**, 1716–1723, and references cited therein.
12. Kühn, F. E.; Groarke, M.; Bencze, E.; Herdtweck, E.; Prazeres, A.; Santos, A. M.; Calhorda, M. J.; Romão, C. C.; Gonçalves, I. S.; Lopes, A. D.; Pillinger, M. *Chem. Eur. J.* **2002**, *8*, 2370–2383.
13. Frisch, M. J.; Trucks, G. W.; Schlegel, H. B.; Scuseria, G. E.; Robb, M. A.; Cheeseman, J. R.; Zakrzewski, V. G.; Montgomery, J. A.; Stratmann, R. E.; Burant, J. C.; Dapprich, S.; Millam, J. M.; Daniels, A. D.; Kudin, K. N.; Strain, M. C.; Farkas, O.; Tomasi, J.; Barone, V.; Cossi, M.; Cammi, R.; Mennucci, B.; Pomelli, C.; Adamo, C.; Clifford, S.; Ochterski, J.; Petersson, G. A.; Ayala, P. Y.; Cui, Q.; Morokuma, K.; Malick, D. K.; Rabuck, A. D.; Raghavachari, K.; Foresman, J. B.; Cioslowski, J.; Ortiz, J. V.; Stefanov, B. B.; Liu, G.; Liashenko, A.; Piskorz, P.; Komaromi, I.; Gomperts, R.; Martin, R. L.; Fox, D. J.; Keith, T.; Al-Laham, M. A.; Peng, C. Y.; Nanayakkara, A.; Gonzalez, C.; Challacombe, M.; Gill, P. M. W.; Johnson, B. G.; Chen, W.; Wong, M. W.;

- Andres, J. L.; Head-Gordon, M.; Replogle, E. S.; Pople, J. A. *GAUSSIAN 98* (Revision A.1), Gaussian, Inc.: Pittsburgh, PA, **1998**.
14. Hay, P. J.; Wadt, W. R. *J. Chem. Phys.* **1985**, 82, 270-283.
  15. Dunning Jr., T. H.; Hay, P. J. In *Modern Theoretical Chemistry*; Schaefer, H. F., Ed.; Plenum: New York, **1976**; Vol. 3, pp. 1-28.
  16. NIST Computational Chemistry Comparison and Benchmark Database, NIST Standard Reference Database Number 101, Release 12, Aug 2005, Editor: Russell D. Johnson III, <http://srdata.nist.gov/cccdb>.

*Sample availability:* Compounds **1** and **2** are available from the authors on request.

© 2006 by MDPI (<http://www.mdpi.org>). Reproduction is permitted for noncommercial purposes.